

## Femtosecond laser-induced cone emission in dense cesium vapor

D. Aumiler, T. Ban, and G. Pichler

*Institute of Physics, Bijenička 46, P.O. Box 304, HR-10001 Zagreb, Croatia*

(Received 26 November 2004; published 13 June 2005)

We report the observation of cone emission generated when  $\sim 10$ -nJ, 100-fs laser pulses in the 730–770 nm wavelength range are transmitted through a dense cesium vapor. The spatial and spectral characteristics of the observed cone emission were studied experimentally. Cone angle dependence on the laser wavelength, laser average power, and Cs atomic and molecular concentrations were investigated. The cone emission (CE) was only observed when the laser beam self-focused after passing through the medium. We identify the self-phase modulation as a dominant mechanism for CE generation in our experiment.

DOI: 10.1103/PhysRevA.71.063803

PACS number(s): 42.65.Jx, 33.80.-b, 42.65.Re

### I. INTRODUCTION

Since the early 1970s, the phenomenon referred to as conical or cone emission (CE) has been widely investigated in literature. Several different models were proposed to explain numerous experimental results. However, none of these models offer a general physical interpretation of the observed phenomena. As a complex phenomenon of an intense light beam interacting with a nonlinear medium, it seems reasonable to suspect that CE can arise by different physical reasons in different experimental conditions.

CE was observed both in resonance and nonresonance media. In most of the published papers, the CE in resonance media was observed as a diffuse ring of light appearing around a central laser spot when an intense laser beam, blue detuned with respect to an atomic resonance, propagates through a vapor. The CE spectrum is redshifted with respect to the atomic transition involved. CE in atomic vapors using pulsed nanosecond (ns) lasers was observed in sodium [1–5], potassium [6], cesium [7], barium [7–9], calcium [10], and strontium [11,12] vapor. CE using a cw laser was observed in sodium [13].

The usual interpretation of CE is based on four-wave mixing (FWM) of Rabi sidebands and the effects of diffractive spreading during propagation [3,12,13]. It was also reported in these papers that self-focusing occurs simultaneously with Rabi sideband generation leading to the formation of stable self-trapped filaments of light. Self-focusing takes place as nonlinear, intensity-dependent, refractive index gradients overcome beam diffraction. According to the optical Kerr-law description, self-induced refractive index gradients grow linearly with laser intensity [6], i.e.,  $n = n_0 + n_2 I$ , where  $n$  and  $I$  are the refractive index and laser intensity, respectively. Under these conditions spatial and spectral structure of the emitted radiation is greatly modified by the self-focusing process [14,15]. The CE then occurs red detuned from the atomic resonance line (low-frequency Rabi sideband) at about the angle given by either a phase-match condition or refraction at the boundary of the filament, whereas the high-frequency Rabi sideband is trapped within the filament. However, Hart *et al.* [11] reported on the failures of the four-wave mixing model for CE. A blueshifted cone was observed in their experiment whose frequency is inconsistent

with the FWM. Their results have indicated that FWM and boundary refraction propagation effects are insufficient for an accurate description of CE. A time-dependent theory for CE during near-resonant propagation of laser light in an atomic vapor, which includes full propagation for the laser and frequency sidebands in a nonlinear two-level medium, is presented in Ref. [16].

A Cherenkov-type emission has also been invoked to explain the CE phenomenon [17]. This effect is intrinsically quantum in nature and comes from the spatial correlation of the medium polarization generated by spontaneous emission and is in many ways analogous to a spontaneous four-wave mixing. The in-phase polarization of the medium acts as a Cherenkov-type source for the two beams (blue- and redshifted with respect to the atomic resonance). A phase-matching condition similar to the Cherenkov condition was obtained in Ref. [18]. In that paper CE is described as a directional superfluorescence that follows from the cooperative effects and was found that the blueshifted cone can appear only for extremely strong laser intensities.

Ter-Mikaelian *et al.* [7] observed the CE in cesium and barium vapor. In contrast to other CE experiments, they reported no frequency shift of the CE spectra relative to the laser pumping frequency. They interpreted this CE as being due to the spatial self-phase modulation. As a result of spatial self-phase modulation, different radial intensities pick up different amounts of phase during the propagation through the nonlinear medium, resulting in rings (CE) in the far field.

In our opinion, in any given physical situation all physical mechanisms proposed for the explanation of the CE should be considered, although it is possible that according to particular physical conditions one or the other might dominate. Therefore, although numerous papers have been written on the subject, the question of a full and consistent theory for the CE generation still remains unresolved.

In the present work we report the observations of CE in dense cesium vapor induced by femtosecond laser pulses. Sarkisyan *et al.* [19] reported the observation of potassium atomic vapor CE produced by 2-ps laser pulses. The use of 150-fs laser pulses, blue detuned from the potassium resonance line, did not yield CE in their experiment. In our experiment, CE generation was observed in the 730–770-nm laser wavelength range, in the spectral region far from Cs

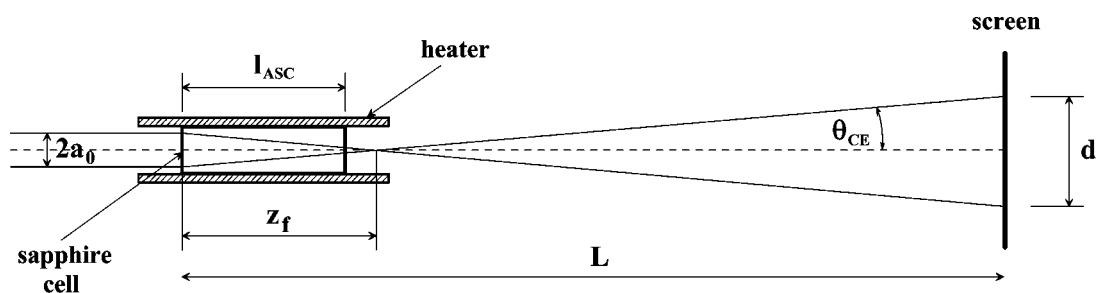


FIG. 1. Experimental geometrical arrangement, not to scale:  $a_0$ , laser beam radius;  $l_{ASC}$ , ASC length;  $L$ , distance from the screen;  $z_f$ , self-focusing length;  $d$ , CE diameter;  $\theta_{CE}$ , CE angle.

atomic resonances. We report experimental evidence of CE generation based on a molecular resonance, thus making a clear distinction from other published CE experiments.

## II. EXPERIMENT

A Tsunami mode-locked Ti:sapphire laser with pulse duration of  $\sim 100$  fs was used in the experiment. The pulse spectrum was close to the transform limit, pulse repetition was 80 MHz, with maximum average power used up to 600 mW. The radial beam profile was Gaussian with  $\sim 2$  mm diameter at  $1/e^2$  intensity and less than 0.5-mrad beam divergence. The laser beam was sent through the cesium vapor cell, without the use of any focusing element, and the light transmitted through the cell was normally incident onto a screen 5.4 m away. In all experimental conditions that led to the CE formation, self-focusing of the laser beam was observed behind the exit of the cell. The CE angle and self-focusing length are calculated from the measurements of the CE diameter on the screen, based on the geometry of our experimental arrangement, shown in Fig. 1. The laser was linearly polarized and CE is polarized in the same direction as the laser, which is consistent with other CE experiments. An Ocean Optics S2000 spectrometer with 1.5-nm resolution was used to record the spectrum at the exit of the cell.

We used a linear all-sapphire cell (ASC) with a length of 162 mm and inside diameter of 10 mm, filled with pure cesium metal. The laser propagation direction was parallel to the optical axis of the sapphire window, thus avoiding birefringent effects. The cesium vapor density was determined from the temperature measured at the center of the cell. Cell temperature range of 600–900 K was investigated. In the used ASC the superheating of cesium vapor is possible. By raising the temperature of the cell, Cs density raises according to the vapor pressure curve. The amount of cesium metal filled in the cell is arranged in such a way that above a certain temperature there is no liquid cesium left to evaporate. Additional heating above this critical temperature  $T_c$  ( $\sim 710$  K in our experimental conditions) can only lead to thermal dissociation of  $Cs_2$  molecules (which are always present in the vapor to within a few percent). Cesium atomic ( $N_{Cs}$ ) and molecular ( $N_{Cs_2}$ ) densities at  $T \leq T_c$  are determined from the vapor temperature using the vapor pressure curves

[20] (for a detailed analysis of the density determination in the ASC used, see Ref. [21]). At temperatures above  $T_c$ ,  $N_{Cs}$  remains essentially constant, whereas  $N_{Cs_2}$  decreases due to superheating [22,23] and is given by [24]

$$N_{Cs_2}(T) = N_{Cs_2}(T_c) \sqrt{\frac{T}{T_c} \left[ \frac{D}{k} \left( \frac{1}{T} - \frac{1}{T_c} \right) \right]}, T > T_c. \quad (1)$$

$D=3648$  cm $^{-1}$  [25] is the dissociation energy of the  $Cs_2$  ground state and  $k$  is the Boltzmann's constant. The accuracy of atomic and molecular density determination was within 20%.

The effect of superheating is evident in the measured absorption spectra of Cs vapor shown in Fig. 2. For  $T > T_c$ ,  $Cs_2X \rightarrow D$  and  $X \rightarrow C$  absorption coefficients decrease with increasing temperature (bound-bound transitions with absorption coefficients proportional to  $N_{Cs_2}$ ), whereas there is no significant change in the  $Cs_2$  diffuse band absorption coefficient (predominately free-bound transitions with

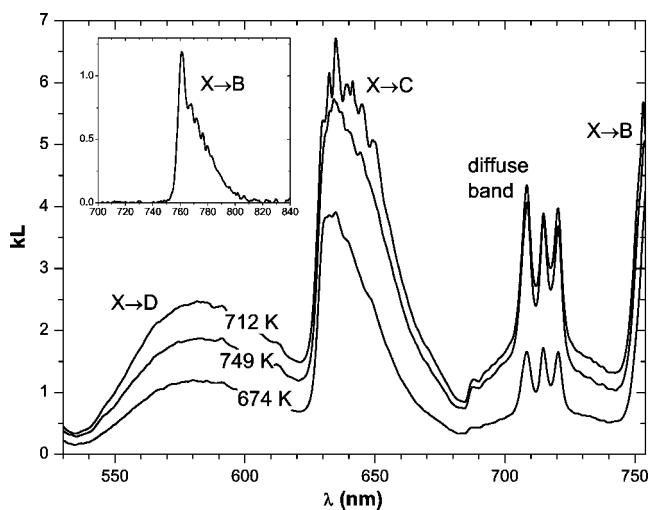


FIG. 2. Cs vapor absorption spectra at  $T < T_c$  ( $T=674$  K),  $T \approx T_c$  ( $T=712$  K), and  $T > T_c$  ( $T=749$  K) (strong  $Cs_2X \rightarrow B$  absorption band makes the vapor completely opaque above 750 nm at these temperatures); inset:  $Cs_2X \rightarrow B$  band absorption spectrum at  $T = 509$  K.

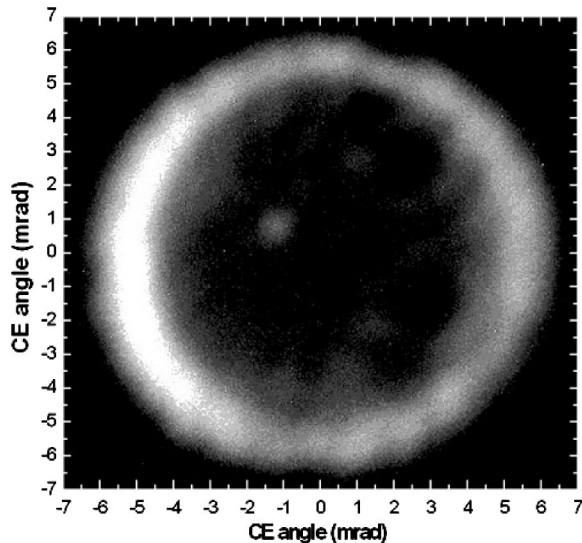


FIG. 3. Image of the cone emission angular distribution as seen on the screen.

absorption coefficient proportional to  $N_{\text{Cs}}^2$ ). For the vapor temperatures shown in Fig. 2, strong  $\text{Cs}_2X \rightarrow B$  absorption band makes the vapor completely opaque above 750 nm.  $\text{Cs}_2X \rightarrow B$  absorption coefficient at a lower temperature is presented as an inset in Fig. 2.

### III. RESULTS

An example of a typical CE angular distribution is shown in Fig. 3. The most distinct feature is the absence of the central laser spot, which is usually present in all other CE experiments. In addition, CE has a small angular spread of  $\Delta\theta/\theta \approx 0.15$ , compared with  $\Delta\theta/\theta \approx 0.3$  from pulsed nanosecond experiments and similar to  $\Delta\theta/\theta \approx 0.1$  from the picosecond experiment [19].

The results of the CE angle dependence on the cell temperature are shown in Fig. 4. At cell temperatures below 600 K, there is no significant effect of the medium on the laser beam. Above 600 K, after passing through the cell, the laser beam appears with angular distribution typical for the conical emission (one ring pattern). The CE angle increases as cell temperature is increased and reaches its maximum value at about 710 K, which corresponds to the critical temperature  $T_c$  for superheating of the cesium vapor in the cell. Further increase of the cell temperature leads to a gradual decrease of the CE angle. Cs atomic and molecular concentrations in the measured temperature range are shown in inset graphs in Fig. 4. There is an apparent correlation of the CE angle and the density of  $\text{Cs}_2$  molecules. Therefore we conclude that the CE observed in our experiment is of molecular origin. To support this idea, we note that CE was observed in the 730–770-nm laser wavelength range, the spectral region where partial overlap with  $\text{Cs}_2X \rightarrow B$  absorption band exists (see Fig. 2).

In the nanosecond experiments, the CE angle dependence  $\theta \propto N^{1/2}$  has been almost universally observed, where  $\theta$  refers to the CE angle and  $N$  to the density of the resonance atoms.

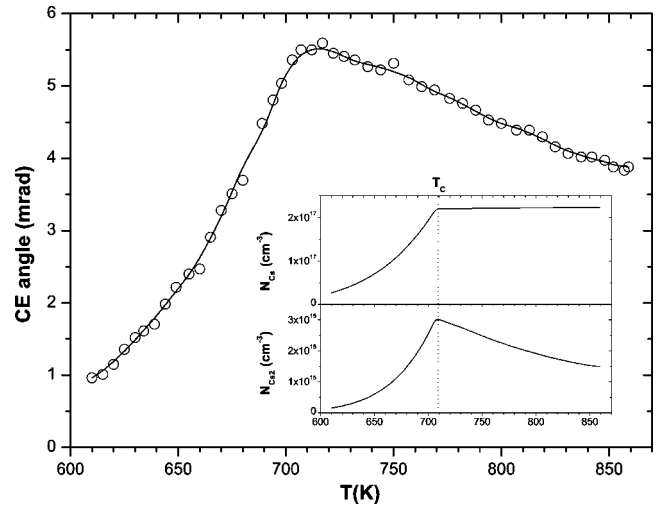


FIG. 4. CE angle as a function of cell temperature ( $\lambda_{\text{laser}} = 756 \text{ nm}$ ,  $P_{\text{laser}} = 580 \text{ mW}$ ). Inset: Cs and  $\text{Cs}_2$  concentrations in the same temperature range.

The picosecond experiment states  $N^{0.4}$  CE angle dependence. Since in our experiment the CE angle exhibits the same behavior as  $N_{\text{Cs}_2}$  we investigated the CE angle dependence on  $\text{Cs}_2$  molecular density. Our data fit to  $\theta \propto N_{\text{Cs}_2}^{0.6}$  in the  $T \leq T_c$  temperature region, and  $\theta \propto N_{\text{Cs}_2}^{0.5}$  for  $T > T_c$ . The two obtained values agree within 20% uncertainty given by the uncertainty in molecular density determination.

The CE was only observed when self-focusing of the laser beam occurred after passing through the cell. The CE angle dependence on laser power is shown in Fig. 5. The CE angle increases linearly for  $P_{\text{laser}} \leq 300 \text{ mW}$ , reaches the maximum value at  $P_{\text{laser}} \approx 400 \text{ mW}$ , and then saturates. The input average power is the laser power incident on the vapor, corrected to account for  $\sim 8\%$  window reflection loss. In addition, self-focusing length dependence on laser power is also shown in Fig. 5. The measured data are fitted to the relation for the self-focusing length of a Gaussian beam [26]:

$$z_f = \frac{0.367\kappa a_0^2}{\sqrt{\left(\sqrt{\frac{P_{\text{laser}}}{P_C}} - 0.852\right)^2 - 0.0219}}, \quad (2)$$

where  $z_f$  is the self-focusing length,  $P_C$  is the critical power for self-focusing,  $\kappa$  is the wave vector, and  $a_0$  is the initial beam radius. The values for critical power for self-focusing obtained from the fit are  $P_C = 36 \pm 4 \text{ mW}$  and  $P_C = 39 \pm 2 \text{ mW}$  at  $T = 681 \text{ K}$  and  $T = 860 \text{ K}$ , respectively. The obtained  $P_C$  values agree within the quoted errors, meaning that  $P_C$  has the same value at  $T = 681 \text{ K}$  and  $T = 860 \text{ K}$ . These two temperatures correspond to the same value of the  $\text{Cs}_2$  molecular concentration, whereas the Cs atomic concentrations are different (see Fig. 4.). Therefore the critical power for self-focusing (i.e., the nonlinear refractive index  $n_2$ ) in our system is given by the  $\text{Cs}_2$  molecular concentration. On this account, the molecular origin of the observed CE is confirmed. From the measured critical power for self-focusing we estimated the nonlinear refractive index  $n_2$

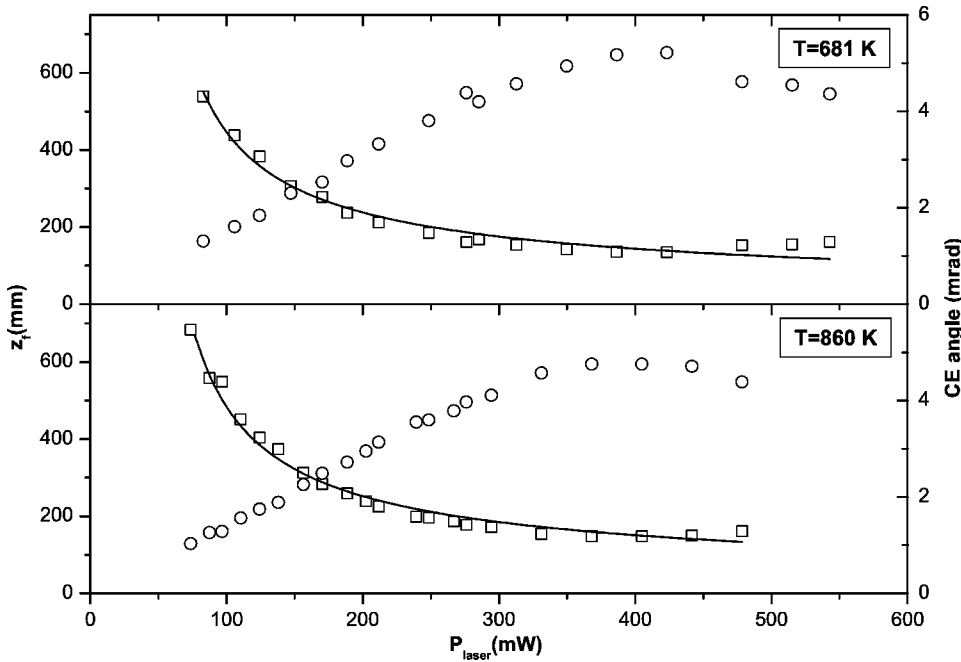


FIG. 5. The CE angle (circles) and self-focusing length (squares: experimental data; line-fit result) as a function of laser average power at  $T=681$  K and  $T=860$  K;  $\lambda_{\text{laser}} \approx 754$  nm.

$\approx 1.5 \times 10^{-13}$  cm<sup>2</sup>/W [27]. The resulting spectral broadening of the laser pulse, due to the self-phase modulation, is about 30% (this results in 1.8-nm broadening of the laser spectrum in the measurements shown in Fig. 6).

The CE spectra for fixed laser wavelength, taken at two different cell temperatures ( $T < T_c$  and  $T \approx T_c$ ), are shown in Fig. 6. In addition to the CE spectra, the optical thickness of cesium vapor at given temperatures and wavelength range of interest are also shown. As can be seen from the figure, CE spectra are strongly modified by the Cs<sub>2</sub>X-B absorption. The observed CE spectra can be interpreted as the blue wing of the laser spectrum (broadened by self-phase modulation) which is not absorbed in the optically thick medium.

The CE angle dependence on laser wavelength is shown in Fig. 7. For given experimental conditions, the CE angle

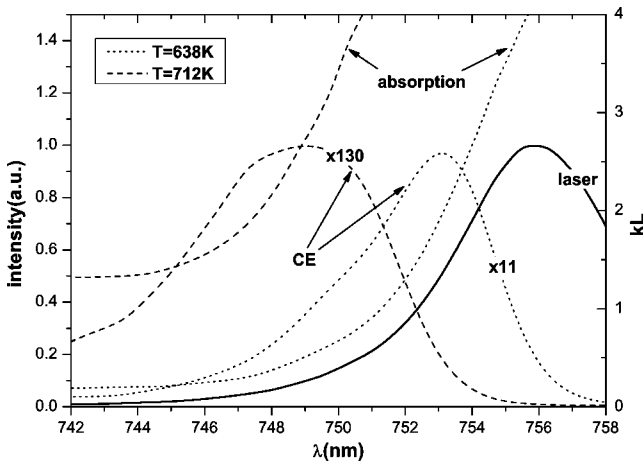


FIG. 6. The CE spectra taken at  $T < T_c$  ( $T=638$  K) and  $T \approx T_c$  ( $T=712$  K); left ordinate refers to the laser and CE spectral intensity (the CE intensity at  $T=638$  K and  $T=712$  K is multiplied by a factor of 11 and 130, respectively), right ordinate refers to cesium vapor optical thickness at given temperatures.

maxima are observed for the laser wavelength of about 754 nm. This comes as a result of changes in the nonlinear refractive index  $n_2$  and absorption coefficient, as the molecular resonance (connected with the maximum of the Cs<sub>2</sub>X-B band positioned at 761 nm) is approached (see Fig. 2).

The CE average power increases linearly with input laser average power, as shown in Fig. 8. CE has a conversion efficiency of up to 24% (depending on the experimental conditions), which is considerably higher than reported in any other CE experiment. The CE average power is that incident on the exit window of the cell (the exit CE power is corrected to account for exit window loss).

#### IV. DISCUSSION

The existence of self-focusing seems to be crucial for the generation of cone emission in our experiment. CE was only observed when the laser beam self-focused after passing through the cell. We suggest that self-phase modulation is a dominant mechanism for the CE generation in our experiment. Several experimental results support this idea. First, no CE spectrum frequency shift relative to the laser was observed. As a result of the propagation in the nonlinear medium the laser spectrum broadens about 30% (due to self-phase modulation). Simultaneously, due to the abrupt change of the Cs<sub>2</sub>X-B absorption coefficient in the spectral region of interest, only the far blue wing of the broadened laser spectrum remains unabsorbed after passing through the cell and results in the observed CE spectrum. Second, CE is observed as a one-ring pattern without the central laser spot. This is a result of the spatial refractive index gradients (optical Kerr effect) which induce phase differences across the radial beam profile, thus resulting in a far-field ring pattern (one ring is observed when the phase difference induced is less than  $2\pi$  [7]). Third, high laser-CE energy conversion of up to 24% (depending on the experimental conditions) is observed,

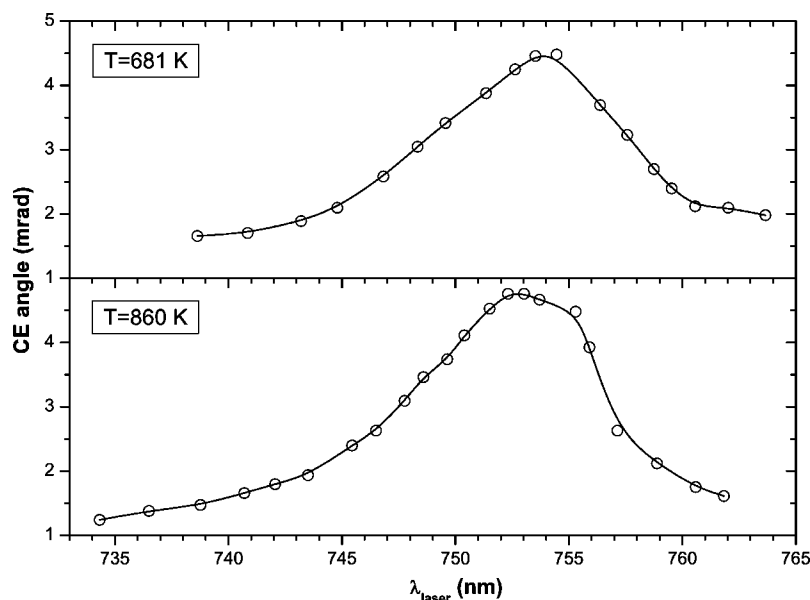


FIG. 7. The CE angle as a function of laser wavelength at  $T=681$  K and  $T=860$  K;  $P_{\text{laser}} \approx 550$  mW.

since CE in fact represents the partially absorbed, self-phase modulated laser pulse. Finally, CE average power increases linearly with input laser average power.

Linear dependence of CE power on the input laser power rules out the four-wave mixing process as a physical mechanism responsible for the CE generation in our experiment. Additionally, neither red nor blue sideband generation have been observed in the measured CE spectra, contradictory to the FWM and Cherenkov-type process. As an important distinction from other CE experiments in which CE is induced by resonance one- or two-photon excitation of an atomic two-level system, we associate the CE generation with the strong molecular resonance connected with the maximum of the  $\text{Cs}_2$ X-B band positioned at 761 nm.

CE observations in our experiment seem to be consistent with the self-phase modulation model for the CE generation proposed by Ter-Mikaelian *et al.* [7]. Their work considers pulse propagation without dispersion in nonabsorbing atomic vapor, in the conditions when self-focusing is negligible.

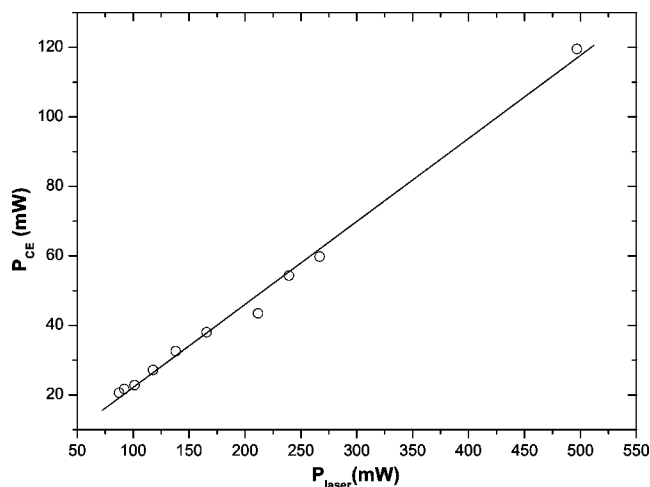


FIG. 8. The CE average power as a function of laser average power;  $T=701$  K,  $\lambda_{\text{laser}}=750$  nm.

However, these assumptions are not applicable to our experimental conditions, so any quantitative analysis of our experimental data based on their model is not applicable. The complete physical description of CE generation in our experiment should take into account the ultrashort laser-pulse propagation effects in a nonlinear, near-resonance medium. The full theoretical treatment of our medium, which is highly optically thick  $\text{Cs}_2$  molecular vapor, is a very complex task.

We would like to point out that we have recently observed femtosecond laser-induced CE in dense rubidium vapor. CE in rubidium vapor occurs when the laser is blue and red detuned from the centers of the Rb  $D_1$  and  $D_2$  first resonance lines. We are currently working on a full time-dependent theory for CE during near-resonant propagation of femtosecond laser light in the nonlinear rubidium two-level atomic vapor. Additionally, we suspect that the laser-pulse repetition could also play an important role in the interpretation of the femtosecond laser-induced CE. It was recently found that a train of pulses from a femtosecond mode-locked laser can lead to the accumulation in both population and coherence of an atomic system [28,29].

### V. CONCLUSION

We report the observation of the femtosecond laser-induced cone emission in dense cesium vapor. CE was observed in the  $2.7 \times 10^{16}$ – $2.2 \times 10^{17}$   $\text{cm}^{-3}$  Cs atomic density range ( $1.5 \times 10^{14}$ – $3 \times 10^{15}$   $\text{cm}^{-3}$   $\text{Cs}_2$  molecular density range), with the use of  $\sim 100$ -fs laser pulses in the 730–770-nm wavelength range and average laser power of 50–600 mW. The CE angles up to 6 mrad and conversion efficiency of up to 24% were observed, depending on cell temperature, laser wavelength, and laser power as input parameters.

Based on the possibility of generation of superheated cesium vapor (i.e., the thermal dissociation of  $\text{Cs}_2$  molecules), a direct correlation of the  $\text{Cs}_2$  molecular density and CE

angle was observed, leading to the conclusion of the molecular origin of CE. The CE angle maximum appears for laser wavelength in the 750–755-nm spectral region, corresponding to the abrupt change of the  $\text{Cs}_2\text{X-B}$  absorption coefficient. The measurements of the self-focusing length dependence on laser power also support the molecular origin of CE, since the obtained critical power for self-focusing is determined by the  $\text{Cs}_2$  molecular density.

We identify the self-phase modulation as a dominant mechanism for CE generation in our experiment and point out problems involved in a quantitative analysis of our mea-

sured data. We also report our preliminary results in the field of femtosecond laser-induced CE in rubidium vapor and stress the reasons for further investigation of this intriguing and complex phenomenon.

#### ACKNOWLEDGMENTS

We acknowledge support from the Ministry of Science and Technology of Republic of Croatia, European Commission Research Training Network (FW-5), and Alexander von Humboldt Foundation.

- 
- [1] A. Dreischuh, V. Kamenov, S. Dinev, U. Reiter-Domiati, D. Gruber, and L. Windholz, *J. Opt. Soc. Am. B* **15**, 34 (1998).
- [2] A. Dreischuh, U. Reiter-Domiati, D. Gruber, L. Windholz, and S. Dinev, *Appl. Phys. B: Lasers Opt.* **66**, 175 (1998).
- [3] D. Harter and R. Boyd, *Phys. Rev. A* **29**, 739 (1984).
- [4] D. J. Harter, P. Narum, M. G. Raymer, and R. W. Boyd, *Phys. Rev. Lett.* **46**, 1192 (1981).
- [5] I. Golub, G. Erez, and R. Shuker, *J. Phys. B* **19**, L115 (1986).
- [6] D. Grischkowsky, *Phys. Rev. Lett.* **24**, 866 (1970).
- [7] M. Ter-Mikaelian, G. Torossian, and G. Grigoryan, *Opt. Commun.* **119**, 56 (1995).
- [8] C. H. Skinner and P. D. Kleiber, *Phys. Rev. A* **21**, 151 (1980).
- [9] W. Chalupczak, W. Gawlik, and J. Zachorowski, *Phys. Rev. A* **49**, 4895 (1994).
- [10] M. Fernandez-Guasti, J. Hernandez-Pozos, E. Haro-Poniatowski, and L. Julio-Sanchez, *Opt. Commun.* **108**, 367 (1994).
- [11] R. Hart, L. You, A. Gallagher, and J. Cooper, *Opt. Commun.* **111**, 331 (1994).
- [12] B. Paul, M. Dowell, A. Gallagher, and J. Cooper, *Phys. Rev. A* **59**, 4784 (1999).
- [13] J. F. Valley, G. Khitrova, H. M. Gibbs, J. W. Grantham, and Xu Jiajin, *Phys. Rev. Lett.* **64**, 2362 (1990).
- [14] M. L. Dowell, R. Hart, A. Gallagher, and J. Cooper, *Phys. Rev. A* **53**, 1775 (1996).
- [15] M. L. Dowell, B. D. Paul, A. Gallagher, and J. Cooper, *Phys. Rev. A* **52**, 3244 (1995).
- [16] B. D. Paul, J. Cooper, and A. Gallagher, *Phys. Rev. A* **66**, 063816 (2002).
- [17] L. You, J. Mostowsky, J. Cooper, and R. Shuker, *Phys. Rev. A* **44**, R6998 (1991).
- [18] Y. Ben-Aryeh, *Phys. Rev. A* **56**, 854 (1997).
- [19] D. Sarkisyan, B. D. Paul, S. T. Cundiff, E. A. Gibson, and A. Gallagher, *J. Opt. Soc. Am. B* **18**, 218 (2001).
- [20] A. N. Nesmeyanov, *Vapor Pressures of Chemical Elements* (Elsevier, New York, 1963).
- [21] D. Aumiler, T. Ban, R. Beuc, and G. Pichler, *Appl. Phys. B: Lasers Opt.* **76**, 859 (2003).
- [22] T. Ban, H. Skenderović, S. Ter-Avetisyan, and G. Pichler, *Appl. Phys. B: Lasers Opt.* **72**, 337 (2001).
- [23] T. Ban, S. Ter-Avetisyan, R. Beuc, H. Skenderović, and G. Pichler, *Chem. Phys. Lett.* **313**, 110 (1999).
- [24] D. H. Sarkisyan, A. S. Sarkisyan, and A. K. Yalanusyan, *Appl. Phys. B: Lasers Opt.* **66**, 241 (1998).
- [25] H. Weickenmeier, U. Diemer, M. Wahl, M. Raab, W. Demtröder, and W. Müller, *J. Chem. Phys.* **82**, 5354 (1985).
- [26] Y. R. Shen, *The Principles of Nonlinear Optics* (Wiley-Interscience, New York, 1984).
- [27] J. C. Diels and W. Rudolph, *Ultrashort Laser Pulse Phenomena* (Academic, San Diego, 1996).
- [28] D. Felinto, C. A. C. Bosco, L. H. Acioli, and S. S. Vianna, *Opt. Commun.* **215**, 69 (2003).
- [29] A. M. Matthew, C. Stowe, J. R. Lawall, D. Felinto, and J. Ye, *Science* **36**, 2063 (2004).